

FORMATION OF YARDANGS OUT OF WIND-SCULPTED BEDROCK: IMPLICATIONS FOR PLANETARY SURFACES. J. Radebaugh¹, L. Kerber², Dylan McDougall¹, Jonathon Sevy¹, Jason Rabinovitch².

¹Department of Geological Sciences, Brigham Young University, Provo, UT (janirad@byu.edu), ²Jet Propulsion Laboratory, California Institute of Technology, Pasadena, CA.

Introduction: Planetary surfaces dominated by wind and with the presence of positive relief sedimentary, volcanic, precipitate or bedrock deposits yield landscapes carved by wind. The most notable features are regularly spaced ridges termed yardangs [1, 2]. These landforms are also found on Mars [3, 4], Venus, Titan [5] and in related forms on Pluto [6]. Other features found in wind-eroded landscapes include undulatory surfaces found in interdune clays [7] and sastrugi [8], formed out of snow sintered into harder firn [9].

The regular spacing of yardangs, and hence their general origins, have been difficult to explain. They are postulated to have formed out of preexisting fluvial channels [10] subsequently exploited by wind or initiated from hydrothermally hardened fractures [11]. There are strong examples of both of these cases.

We argue from observations in the high elevation, hyperarid Puna of Argentina that decameter-scale (meso) yardangs can form spontaneously out of a uniform bedrock surface by the action of wind. This has implications for conditions expected in planetary yardang-bearing surfaces.

Puna Region: The Puna of Argentina is a high-elevation, hyperarid desert dominated by young ignimbrites [11], evaporite basins and young basalt cinder cones. The ignimbrite deposits are widespread, and often contain up to km-scale (mega) yardangs, which do show evidence of fluvial and mass wasting processes in their formation [11]. The youngest and softest [12] ignimbrite, called the Campo de Piedra Pomez (CPP), contains abundant mesoyardangs. These are formed in two main deposits, a white deposit in the SE that has a rigid matrix and abundant pumice and lithics, and a tan deposit found on the NW that has resistant pumice in a softer matrix [12]. Both were visited in field campaigns in 2018 and 2019 by the authors.

Key Observations: In both main areas of the Campo de Piedra Pomez, large, undulatory deposits free of yardangs were found that contained total elevation differences of ~2 m and separated by 5-10 m (Fig. 1). These bore arcuate ridges that trended perpendicular to the wind direction as determined by yardangs in adjacent portions of the fields, and were also noted in other field studies [13]. These undulations had downwind sloping surfaces altered to a darker color and not as wind scoured as the lighter surface (Fig. 1). The ridges were occasionally capped by gravels, sometimes which were cored by sand and fines. These appear to have helped to preserve rare moisture, leading to alteration

(Fig. 2). However, large swaths (several kilometers in all directions) did not bear evidence of gravels and yet their downwind slopes were altered (Fig. 1).



Fig. 1. Undulatory ridged surface in tan deposits with altered downwind slopes (see Fig. 2 for scale).



Fig. 2. Top of undulatory ridge capped in gravels that had moved.



Fig. 3. Undulatory surface with downwind fluting.

In the tan field, the undulatory surfaces attained fluting aligned with the wind direction along the lower elevation portions of the ridges. This morphology is reminiscent of the fluting observed in sastrugi as it progresses along the erosion path [7] (Fig. 3). Farther downwind in the tan field, the fluting became enlarged and deepened into troughs. Once the relative height difference between ridges and troughs reached 1 m, the high portion emerged from the saltation layer and became what we propose is an incipient yardang (Fig. 4).



Fig. 4. Incipient yardang – high ridge with adjacent trough (behind Jonathon).



Fig. 5. Fully formed yardang, with undercut prow (people under for scale)

Farther downwind the undulations and flutes had grown in height and spacing to become isolated promontories separated by troughs - full-fledged yardangs (Fig. 5). Here, the cap is no longer in the saltation zone, and the lower portion is actively being undercut.

The back slopes of fully formed yardangs in both the white and tan deposits are similar to those of the downwind slopes of the undulatory bedrock - $\sim 10^\circ$ [14]. In addition, the back slopes are all dark in color and sometimes have mud crack-like morphologies, indicating alteration by water (Figs. 6, 7).

Formation stages: Based on our observations in the Puna, we list the following sequence for mesoyardang formation: 1 – undulatory surface in bedrock forms (how is not determined here). 2 – downwind slopes receive less wind scouring, more exposure to elements,

perhaps aided by gravels. 3 – fluting forms and extends downwind along low portions of ridges. 4 – flutes enlarge and deepen into troughs. 5 – elevated portions become isolated ridges now yardangs, wind erosion is concentrated in troughs and on front of ridges.



Fig. 6. Yardangs in the white CPP, showing alteration and similar slopes (10) to the downwind caps.

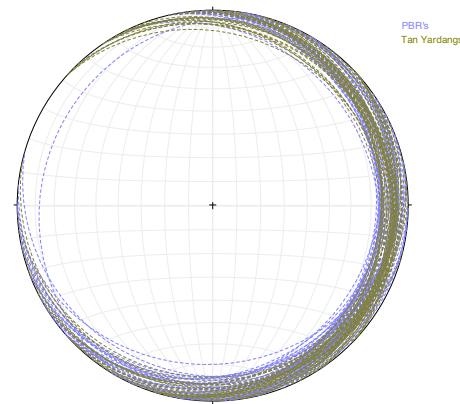


Fig. 7. Dip measurements of undulatory ridges (“PBRs” blue) and windward sides of tan yardangs (brown).

Discussion and Conclusions: We have developed a formation model for yardangs based on our observations of mesoyardangs in the Puna. The conditions here are simple, which makes this a valuable base model to which more complicated conditions can be applied. Yardangs on other planetary surfaces need, at a primary level, wind and a uniform, elevated base. Variations in yardang morphologies should indicate controls beyond these primary constraints, such as material properties and atmospheric conditions.

References: [1] Blackwelder (1934). [2] Ward (1979). [3] Greeley and Iverson (1985). [4] Kerber et al. (2011) *Icarus* 216. [5] Paillou et al. (2016) *Icarus* 270. [6] Moores et al. (2017) *Nature* 541. [7] Radebaugh et al. (2020) LPSC. [8] Kochanski et al. (2018) AGU. [9] Mather (1982) *Polar Record*. [10] Dong et al. (2012). [11] de Silva S. et al. (2010) *PSS* 58. [12] McDougall et al. (2020) LPSC. [13] Bridges et al. (2015). [14] Sevy et al. (2020) LPSC.